JOURNAL OF NANO- AND ELECTRONIC PHYSICS
Vol. **7** No 4, 04098(7pp) (2015)

ЖУРНАЛ НАНО- ТА ЕЛЕКТРОННОЇ ФІЗИКИ
Том **7** № 4, 04098(7cc) (2015)

Nanostructured (Ti-Zr-Nb)N Coatings Obtained by Vacuum-arc Deposition Method: Structure and Properties

O.V. Maksakova[1], S.S. Grankin[2], O.V. Bondar[1], Ya.O. Kravchenko[1], D.K. Yeskermesov[1,3], A.V. Prokopenko[1], N.K. Erdybaeva[3], B. Zhollybekov[4]

[1] *Sumy State University, 2, Rymskogo-Korsakova St., 40007 Sumy, Ukraine*
[2] *Kharkiv National University of Karazin, 4, Svobody Sq., 61022 Kharkiv, Ukraine*
[3] *D. Serikbaev East Kazakhstan state technical university, 69, Protozanova St., 070004 Ust-Kamenogorsk, Kazakhstan*
[4] *Karakalpak State University, 1, Abdirov St., 742012 Nukus, Usbekistan*

(Received 17 November 2015; published online 24 December 2015)

In the article discusses the results of the deposition of nanostructured coatings obtained by vacuum arc deposition of cathode (Ti-Zr-Nb), and analyzes their structure, morphology, elemental composition, and tribological properties (friction, wear and adhesion). The structural analysis showed the formation of an FCC phase and BCC phase in a small amount (at a chamber pressure $P = 4{\cdot}10^{-3}$ Torr). The results of tribological tests showed that the friction coefficient varies from 0.61 to 0.491, and Vickers hardness from 37 to 44.57 GPa when changing (increasing) the pressure in the chamber. The analysis of the elements in the tracks of friction was studied.

Keywords: Nanostructured (Ti-Zr-Nb)N, Hardness, Physical-mechanical properties, Structure.

PACS numbers: 81.15.Ef, 81.15. – z

1. INTRODUCTION

During the exploitation the surface layer of parts expose to heavy mechanical, thermal and chemical resistance. In most cases the loss of their efficiency from the surface is the result of wear, erosion and corrosion resistant surface. Thus, a significant resource of increasing of parts capacity is to improve the properties of material and increasing their tribological properties.

Application of volume-doped materials is often the uneconomical, and in some cases technically impossible. However, the required results can be achieved by modifying not entire volume, but only the surface layer material, for example, by applying to the working surface of multifunctional coatings having high hardness, wear and heat resistance. Multi-element coating on carbides, borides, nitrides and silicides of transition metals are often used as such coatings [1-4]. The stability of the structure and composition, as well as high performance characteristics of multi-element nitride systems provide the required physical and mechanical characteristics of the surface and makes promising their use as protective films that prevented ingress of harmful impurities in the subsurface layers of products [5, 6]. Currently, methods of ion-plasma deposition of coatings, in particular vacuum arc evaporation and magnetron sputtering are the most widely used [7, 8].

In this paper peculiarities of ion-plasma coatings in vacuum-arc evaporation of multi-element systems based on Ti-Zr-Nb in reactive nitrogen atmosphere and the analysis of their physical and mechanical properties are studied.

2. EXPERIMENTAL

The coatings were formed by vacuum arc deposition. As the vaporized materials used unit-cast target (cathode) on the basis of 30 Ti-35 Zr - 35 Nb (at. %). Coating deposition produced at a pressure of the working gas (molecular nitrogen) $3{\cdot}10^{-4}$, $7{\cdot}10^{-4}$ and $4{\cdot}10^{-3}$ Torr (coating Series A, B and C, respectively). The thickness of coating was 4,0 microns. The samples with size of 15 × 15 × 2,5 mm from steel 12X18H9T with roughness of the original surface $R_a \approx 0{,}09$ microns were selected as a substrates for the deposition of coatings. Deposition parameters as well as the surface roughness after deposition of the coating are given in the Table 1.

Table 1 – Technological parameters of deposition and surface roughness surface (Ti-Zr-Nb) N coatings

Series	Arc current I_d, A	Bias voltage U_{sm}, B	Nitrogen pressure P_N, Torr	Roughness R_a, mcm
A	95	100	3×10^{-4}	1,17
B	95	100	7×10^{-4}	0,54
C	95	100	4×10^{-3}	0,42

The surface morphology, fractographs fracture and track of friction was studied on a Scanning Electron Microscope FEI Nova NanoSEM 450. The elemental composition of the coatings was analyzed with spectra of characteristic X-ray using built-in microscope energy dispersive spectrometer of X-ray system PEGASUS (EDAX). X-ray structural studies of the samples with coatings carried out on a DRON-4 in Cu K_α radiation in pointwise mode with scanning step $2\theta = 0{,}05$ degrees.

The microhardness of the coatings was measured at hardness tester model DM 8 with a load on the indenter 0,05 N. Adhesion-cohesive strength, scratch resistance and the mechanism of degradation of coatings were studied on air using a scratch tester Revetest (CSM Instruments).

The tribological tests were carried out on air in a "ball-disc" on friction drive "Tribometer" (CSM Instruments). To this coating with thickness 4,0 microns was deposited on the surface polished ($R_a = 0{,}088$ microns)

 © 2015 Sumy State University

samples in the form of discs of steel 45 ($HRC = 55$) with a diameter 42 mm and a height of 5 mm. As counterface the ball with diameter 6,0 mm was used, it is made of sintered and certified material – Al_2O_3. The load was 3,0 N, the sliding speed was 10 cm/s. Test conditions conform international standards ASTM G99-959, DIN50324 and ISO 20808.

Roughness and also volume of removed coating material were determined by the cross section of track wear on the surface of a sample with an automated precision contact profilometer model Surtronic 25. The structure of the groove wear coating and wear spots on the balls were examined on optical inverted microscope Olympus GX 51 and the scanning electron microscope Quanta 200 3D. As a result of conducted investigation it were evaluated wear factor [9] of sample with coating and statistical partner (ball) according to methodic [10]:

$$W = \frac{V}{P \cdot l}, \quad (1)$$

where W – wear factor [mm^3/N·m]; V – volume of removed material [mm^3]; P - load [N]; l – friction path [m].

The diameter of ball wear was determined using an inverted microscope optical Olympus GX 71, the volume of removed material on the ball is calculated as:

$$V_{\varnothing} = \pi \cdot h^2 \left(r - \frac{1}{3} h \right), \quad (2)$$

where $h = r - \sqrt{r^2 - (d/2)^2}$ – segment height; d – diameter of wear; r – radius of the ball.

The volume of removed coating material is $V_{II} = s \cdot l_{II}$, where l_{II} – the circumference, s – the cross-sectional area of the path of wear.

3. RESULTS AND DISCUSSIONS

Image surface of the coatings as well as fractographs fracture are shown on Figure 1, 2, data on changes in surface roughness (arithmetic average deviation profile R_a) are showed in the Table 1.

The investigation of the surface morphology shows that increasing the pressure of the reaction gas (nitrogen) in the working chamber leads to reduction the amount and size of particulates, that is especially important at presence in a vacuum chamber the active gases forming a refractory compounds with evaporating material [11, 12-14]. Also, the decrease in the roughness of the coating is observed.

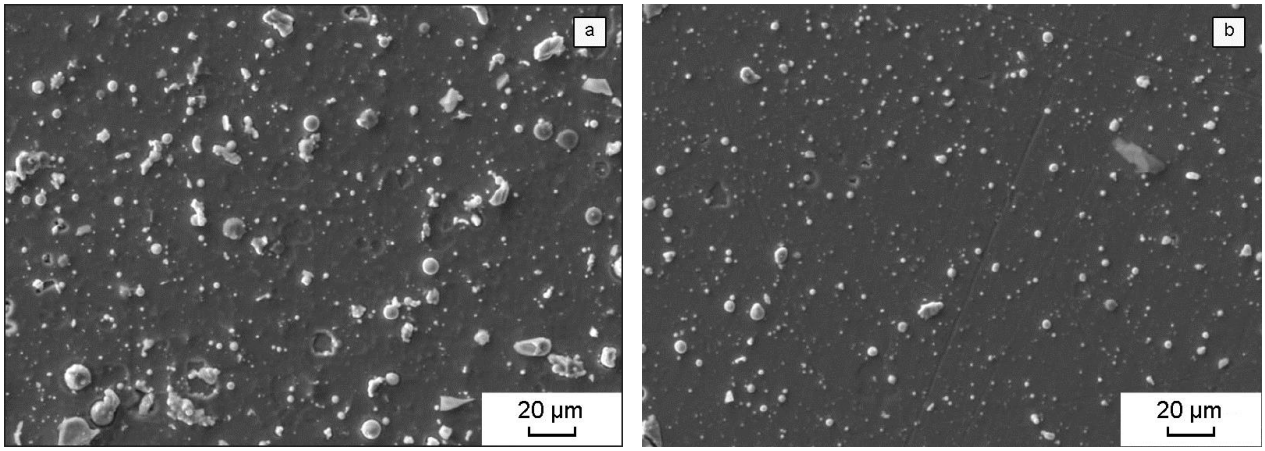

Fig. 1 – Surface (Ti-Zr-Nb) N coatings produced at partial pressure of nitrogen: pressure of nitrogen during deposition $P = 3 \cdot 10^{-4}$ Torr, the surface roughness $R_a = 1{,}17$ microns (a); $P = 4 \cdot 10^{-3}$ Torr, $R_a = 0{,}42$ microns (b)

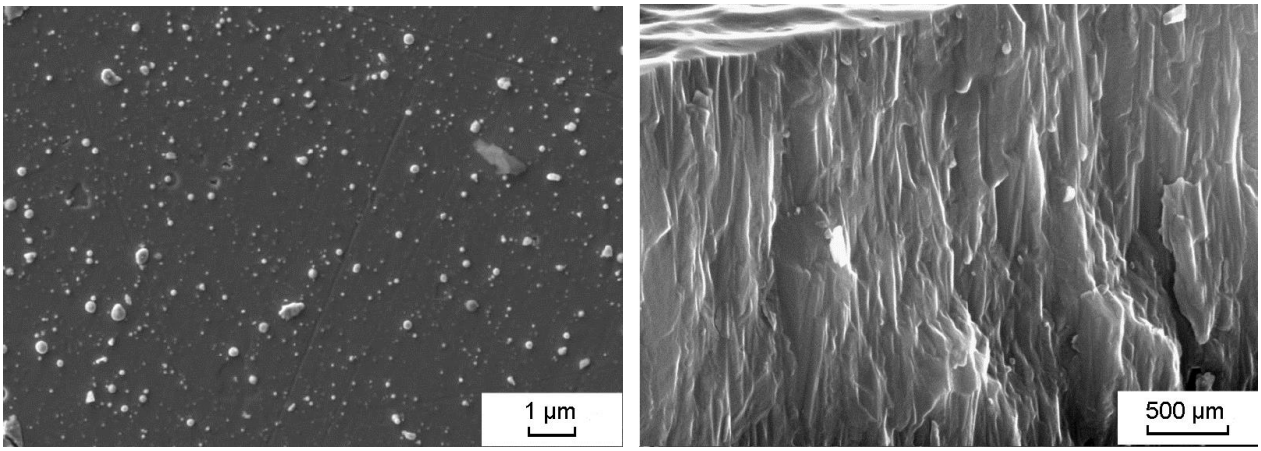

Fig. 2 – Images of fractographs fracture of the coatings (Ti-Zr-Nb) N, obtained at a partial pressure of nitrogen: $P = 4 \cdot 10^{-3}$ Torr

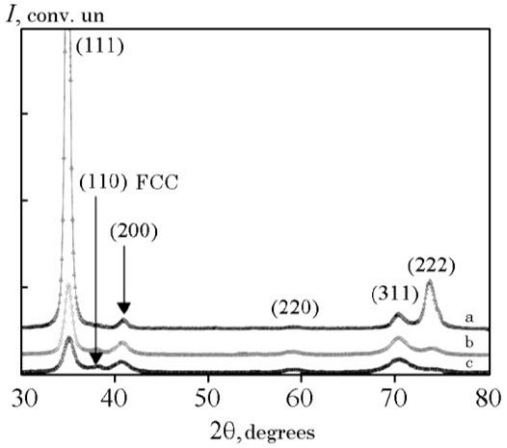

Fig. 3 – Diffractograms of the coatings obtained at different partial pressure of nitrogen: a – $P = 3 \cdot 10^{-4}$ Torr (series A); b – $P = 7 \cdot 10^{-4}$ Torr (Series B); c – $P = 4 \cdot 10^{-3}$ Torr (Series C). Indices of planes without designation refer to FCC phase (Ti-Zr-Nb) N and the indices BCC – to the phase (Ti-Zr-Nb)

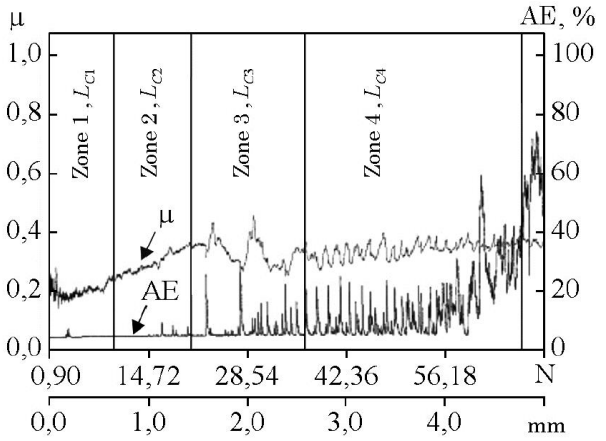

Fig. 4 – Dependence of friction coefficient and acoustic emission signal from the applied load at a scratch test of the coating (Ti-Zr-Nb) N, obtained at a nitrogen pressure of $P = 4 \cdot 10^{-3}$ Torr (sample series B)

The data on the elemental composition of the coatings are presented in the Table 2. As shown, the content of nitrogen and niobium in a series of samples B and C is practically the same, but in the samples obtained at the higher pressure of nitrogen (Series B), the content of the zirconium is higher and titanium is lower than in the samples series B. Increasing the titanium content in the coatings of series B connected, apparently, with a more effective interaction titanium atom with the nitrogen in the subsurface region. Data, summarized in [11, 15-17], on the formation of nitride complexes in the surface region during the deposition of transition metal in the nitrogen atmosphere are lies in the basis of such hypothesis. Ti-N is the most stable among these complexes. The formation of stable nitride complexes significantly reduces the efficiency of spray from growing surface (secondary spraying), that eventually leads to its enrichment with strong nitride-forming element (in this case Ti).

Table 2 – The elemental composition of coatings at. %

Series	Elemental composition, at. %			
	N	Ti	Zr	Nb
A	38,72	20,91	20,38	19,99
B	40,00	22,57	18,04	19,39
C	40,86	20,52	19,36	19,26

The analysis fraktograph fracture coatings obtained under different partial pressures of nitrogen indicates the formation of columnar structure that is character for coatings obtained with vacuum arc deposition (see Fig. 2). From submitted on Figure 3 diffractograms follows that the coating has a FCC structure, but a weak peak at $2\theta = 38°$ indicates the presence of small inclusions with BCC lattice typical for droplet phase formed by vacuum-arc deposition of coatings [12]. With the increasing of pressure of the reaction gas the intensity of this peak decreases probably because of the significant reduction of the content of the droplet phase in the coating, that correlates with the results of surface roughness of the coatings obtained at different pressures (see Fig. 1). A detailed analysis of the elemental composition of the droplet phase of vacuum arc nitride coatings [7] showed that the composition of the droplet phase in the vacuum arc method of evaporation corresponds the melt of evaporated metal target. On the other hand, in [3] demonstrated that the multi-element metal melts from similar 3d-elements form the generalized BCC lattice of substitution during the crystallization. Therefore, the revealed peaks relevant to the BCC lattice naturally associate with formed while the deposition droplet phase, which crystallizes with the formation of BCC lattice of substitution from metal atoms (Ti, Zr, Nb).

By increasing the pressure of the reaction gas it is observe a noticeable increase of the relative intensity of the diffraction peaks from a family of planes {111} cubic FCC lattice nitride phase (Ti-Zr-Nb) N coatings that indicates an increasing of the excellence of preferential orientation growth of crystallites with axis [111] that perpendicular to the plane surface. Defined with method of approximating the size of the crystallites with the increasing of nitrogen pressure increases from 10 nm (at the lowest pressure of $3 \cdot 10^{-4}$ Torr) to 63 nm – at the maximum pressure of $4 \cdot 10^{-3}$ Torr.

The research results of adhesive-cohesive strength and scratch resistance of coatings are shown on Figure 4, 5. By changing the values of the friction coefficient and acoustic emission signal and with the increasing load of scribing (see Fig. 4) the characteristic values of the critical load L_C were determined: L_{C1} – the appearance of the first chevron crack at the bottom and diagonal cracks at the edges of scratches; L_{C2} – forming a plurality chevron cracks at the bottom of the crack and local delamination of coating, the formation of chevron cracks at the bottom of the crack; L_{C3} – cohesive-adhesive destruction of the coating; L_{C4} – plastic abrasion of the coating. As the criterion of the adhesive strength the critical load L_{C4} at which the abrasion of the coating occur was taken.

According to these criteria, the process of destruction of the coating when scratched with the indenter can be divided into four stages. In the load range of $F = 9{,}89$ N to 0,9 N there is a monotonically penetration of the indenter into the coating, herewith the coefficient of friction

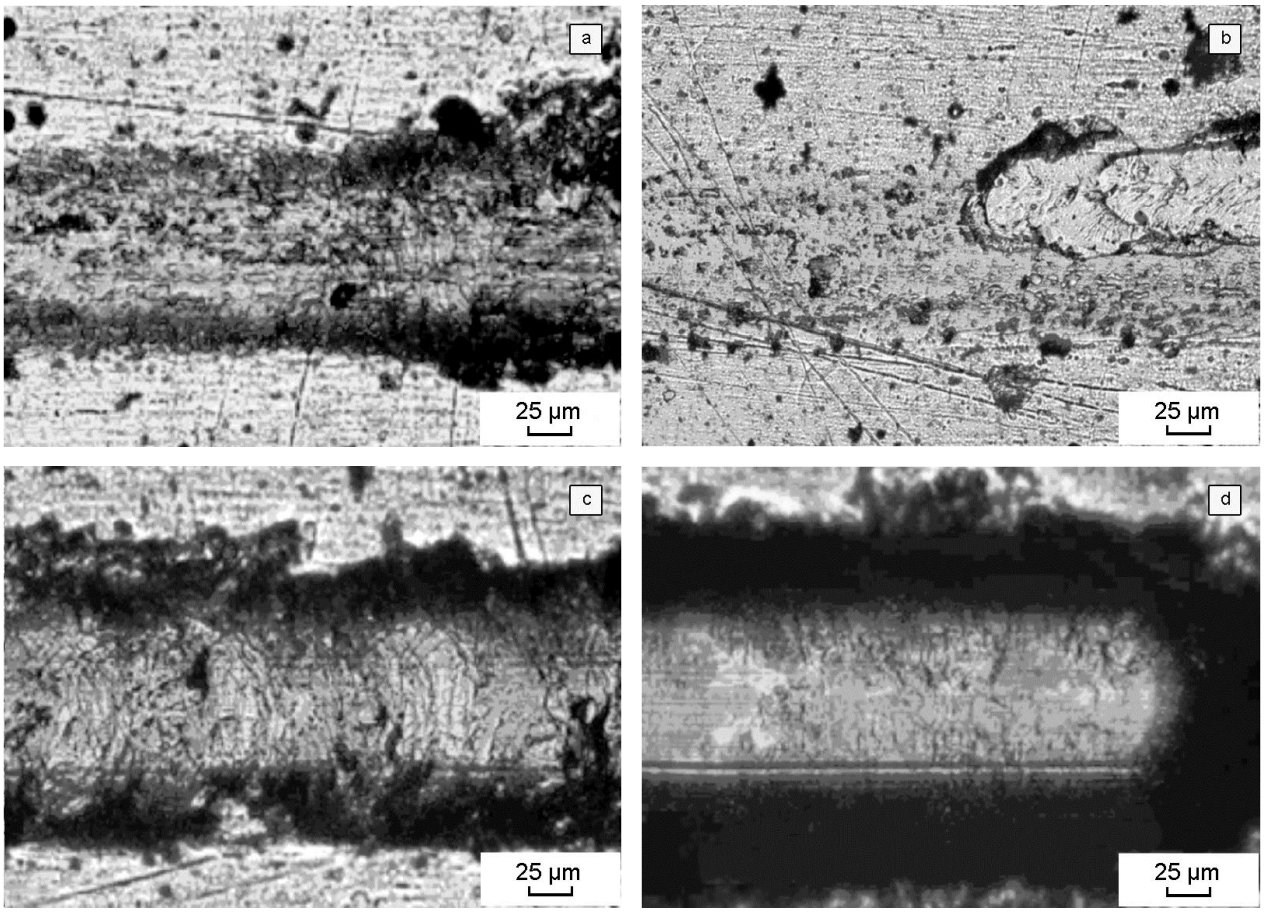

Fig. 5 – Micrographs of the contact area of the diamond indenter with coating (Ti-Zr-Nb) N (sample series B) at different stages of a scratch test (see Fig. 3): Zone 1 (a); Zone 2 (b); Zone 3 (c); Zone 4 (d)

increases slightly, and the signal of acoustic emission preserved unchanged. At the load $F = 15{,}81$ N indenter is completely immersed in the coating, and the slipping of diamond indenter to the cover happens with the friction coefficient 0,35. When the load increases ($F = 20{,}6$-$36{,}4$ N) occurs the extrusion of the material before the indenter in the form of hillocks and increased the penetration depth of the indenter.

In the Table 3 the results of adhesion test of the samples of obtained coatings (Zr-Ti-Nb) N are shown and previously obtained similar data for coatings (Ti-Zr-Si) N and TiN [13] are shown there for comparison. According to [14], the abrasion of the sample during the test on the adhesive strength the most informative characteristics of the destruction are the critical value of the load L_C.

As is known, the most universal parameter that allows to evaluate the mechanical properties of the coating enough rapidity is its micro-hardness [11, 12]. The results of such measurements for the coatings (Zr-Ti-Nb) N are shown in Table 4.

As is seen, the maximum hardness $HV = 44{,}57$ GPa achieved at a pressure of the reaction gas $P = 4 \cdot 10^{-3}$ Torr, and according to [15, 18-21], such coatings can be attributed to superhard ($HV_{0,05} \geq 40$ GPa).

Comparison of profilograms taken from the surface of polished steel discs (substrates), and deposited on them the coatings (Zr-Ti-Nb) N, showing that the coating deposition leads to an increase of surface roughness apparently at the expense of drip compound of the plasma stream.

Table 3 – The results of adhesive tests of the coatings (Zr-Ti-Nb) N, (Ti-Zr-Si) N and TiN

Critical loads	Coatings				
	(Zr-Ti-Nb)N series A	(Zr-Ti-Nb)N series B	(Zr-Ti-Nb)N series C	(Ti-Zr-Si)N	TiN
L_{C1}	2,91	0,9	9,89	3,91	21,31
L_{C2}	29,04	15,82	20,62	18,15	30,91
L_{C3}	43,18	42,37	36,43	24,29	40,28
L_{C4}	59,26	66,24	66,77	43,15	48,84

Table 4 – The average values of microhardness of the coatings based on the system (Zr-Ti-Nb) N

Series	Microhardness, $HV_{0,05}$, GPa
A	37,21
B	40,21
C	44,57

Important parameter that determines the performance of the coatings is also its tribological properties (friction coefficient and wear factor). The coefficient of friction μ defines a cohesive strength rubbing materials and the wear factor – the abrasion resistance (less wear factor, the higher the abrasion resistance)[22-25].

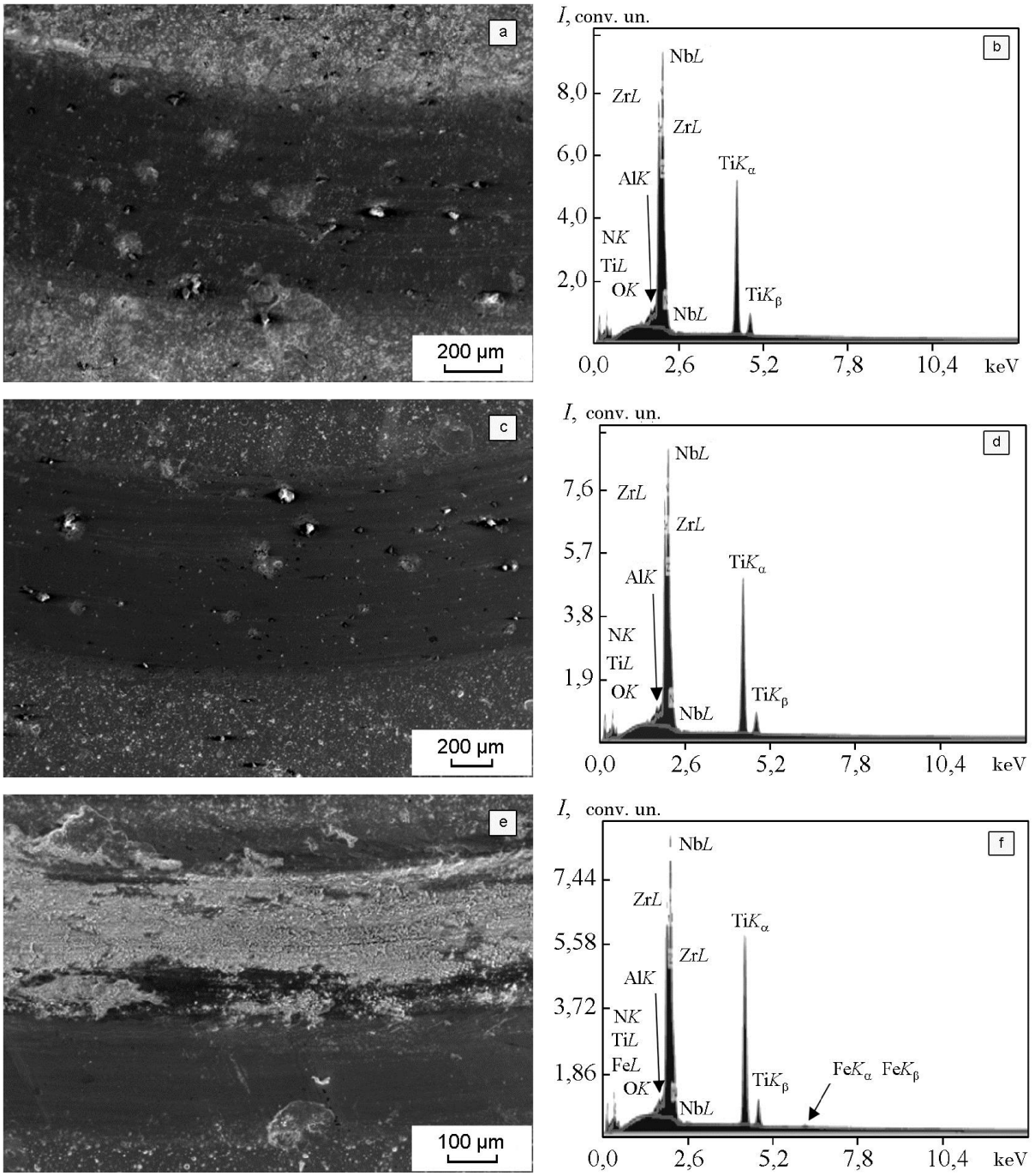

Fig. 6 – Surface of the coating of system (Zr-Ti-Nb) N after the tribological tests (a, c, e) and energy-dispersive spectra of friction tracks (b, d, f): sample the series A (a, b); sample of series B (c, d); sample series B (e, f).

The type of friction tracks and tribological test results are shown on Fig. 6 and in Table 5. The friction coefficient takes values from the initial (at the first contact) to a stationary (column "when tested" in Table 5) at an output at constant value during the test.

On all samples with the coating (series A, B, C) the friction coefficient was higher than 1,0. Such high values may be explained with the high roughness (see Fig. 1), associated with the presence on the surface and in the coating of the droplet fraction formed at vacuum-arc deposition. The appearance of a solid drip component and the formation during the destruction of coating products of wear in the form of particles consisting of hard nitrides, leads to abrasion wear of the coating. The reducing of the surface roughness decreases the friction coefficient from 1,95 to 1,05. With the increasing of the coating hardness the wear factor W of the coating decrease, and the counterface – increased (Table 5).

With the increasing of the pressure and the appearing of preferential orientation of the crystallites growth with the axis [111] (see Fig. 2) it is observed the reduction in capturing and wear material, which correlates with the previously established increasing of hardness with increasing of the nitrogen pressure during the deposition of the coating.

Table 5 – The tribological characteristics of the system "coating (Zr-Ti-Nb) N-Al_2O_3"

Series	Coefficient of friction, μ		Wear factor W, 10^{-5} mm^3/N·m	
	Initial	When tested	Counterface	Sample with coating
A	0,61	1,95	0,391	9,69
B	0,45	1,19	2,84	3,1
C	0,491	1,05	3,21	2,4

The results can be explained with the increasing of the atoms packing density in the plane (111) FCC lattice [12, 26-29], that increases the hardness of the coating, since the introduction of the indenter at the axis of the texture in the coating [111] occurs perpendicular to these planes. The increasing of wear resistance in this case is determined by that fact that during the wear process layer by layer removal of more solid planes (111) material occurs that minimizes its destruction.

4. CONCLUSIONS

Using the method of vacuum arc evaporation unit-cast cathode in the environment of the nitrogen gas reaction nanostructured coating of the systems (Ti-Zr-Nb) N with a clearly pronounced columnar structure were obtained.

The main phase (Zr-Ti-Nb) N that compounds the coating has an FCC lattice. The increasing of the reaction gas pressure leads to the increase of the diffraction peaks from a family of planes {111} that indicates an increase the degree of the preferential orientation growth of crystallites (texture of the axial type) with axis [111] perpendicular to the plane of growth.

The highest microhardness (44,57 GPa) and the wear resistance showed the coatings obtained at a maximum pressure of nitrogen. A formation of (Ti-Nb-Zr) N phase with preferential orientation growth of crystallites with axis [111] perpendicular to the plane of growth is typical for this covering. The power of adhesive destruction in such covering reaches 66,77 Pa.

ACKNOWLEDGEMENTS

This work was done under the aegis of scientificaly-technical collaboration program between Sumy State University (Sumy, Ukraine) and University of Poitiers (Institut P', University of Poitiers, Poitiers, France), and Ukrainian complex state budget programs "Creation of basis of superhard nanostructure coatings fabrication with high physical and mechanical properties" (registration number 0112U001382) and "Physical principles of plasma technologies for complex treatment of multicomponent materials and coatings" (registration number 0113U000137c).

The authors are thankful to Prof. Sobol′ O.V., Prof. Beresnev V.M., Nemchenko U.S, Kolesnikov D.A., prof. Pogrebnjak A.D.

Наноструктурные покрытия (Ti-Zr-Nb)N, полученные методом вакуумно-дугового испарения: структура и свойства

О.В. Максакова[1], С.С. Гранкин[2], А.В. Бондарь[1], Я.О. Кравченко[1], Д.К. Ескермесов[1,3], А.В. Проко-пенко[1], Н.К. Ердыбаева[3], Б. Жоллыбеков[4]

[1] *Сумский государственный университет, ул. Римского-Корсакова, 2, 40007 Сумы, Украина*
[2] *Харьковский национальный университет имени В.Н. Каразина, пл. Свободы 4, 61022 Харьков, Украина*
[3] *Восточно-Казахстанский государственный технический университет имени Д. Серикбаева, ул. Протозанова, 69, 070004 Усть-Каменогорск, Казахстан*
[4] *Каракалпакский государственный университет, ул. Абдирова 1, 742012 Нукус, Узбекистан*

В статье обсуждаются результаты осаждения наноструктурных покрытий,полученных вакуумно-дуговым испарением катода (Ti-Zr-Nb),а также анализируются их структура, морфология, элементный состав и трибологические свойства (трение, износ, адгезия). Структурный анализ показал формирование ГЦК фазы и в небольшом количестве ОЦК-фазы (при давлении в камере $P = 4 \cdot 10^{-3}$ Торр). Результаты трибологических испытаний показали, что коэффицент трения изменяется от 0.61 до 0.491 и твердость по Виккерсу от 37 до 44.57 ГПа, при изменении (увеличении) давления в камере. Проведен анализ элементов в дорожках трения.

Ключевые слова: Наноструктурные (Ti-Zr-Nb)N, Твердость, Физико-механические свойства, Структура.

Наноструктурні покриття (Ti-Zr-Nb)N, отримані методом вакуумно-дугового випаровування: структура та властивості

О.В. Максакова[1], С.С. Гранкін[2], О.В. Бондар[1], Я.О. Кравченко[1], Д.К. Ескермесов[1,3], А.В. Прокопенко[1], Н.К. Ердибаєва[3], Б. Жоллибеков[4]

[1] *Сумський державний університет, вул. Римського-Корсакова, 2, 40007 Суми, Україна*
[2] *Харківський національний університет імені В.Н. Каразіна, пл. Свободи, 4, 61022 Харків, Україна*
[3] *Східно-Казахстанський державний технічний університет імені Д. Серікбаєва, вул. Протозанова, 69, 070004 Усть-Кам'яногірськ, Казахстан*
[4] *Каракалпакський державний університет, вул. Абдирова 1, 742012 Нукус, Узбекистан*

Устатті обговорюються результати осадження наноструктурних покриттів отриманих вакуумно-дуговим випаровуванням катоду (Ti-Zr-Nb), а також аналізується їх структура, морфологія, елементний склад та трибологічні властивості (тертя, знос, адгезія). Структурний аналіз показав формування ГЦК фази та в невеликій кількості ОЦК – фази (при тиску у камері $P = 4{\cdot}10^{-3}$ Торр). Результати трибологічних випробувань показали, що коефіцієнт тертя змінюється від 0.61 до 0.491 та твердість за Віккерсом від 37 до 44.57 ГПа, при зміні (збільшенні) тиску у камері. Проведений аналіз елементів у доріжках тертя.

Ключові слова: Наноструктурні (Ti-Zr-Nb)N, Твердість, Фізико-механічні властивості, Структура.

REFERENCES

1. A.D. Pogrebnjak, Sh.M Ruzimov, *Phys. Lett. A* **120** No 5, 259 (1987).
2. A.D. Pogrebnjak, *J. Nanomater.* **2013**, 780125 (2013).
3. A.D. Pogrebnjak, V.M. Beresnev, A.A. Demianenko, V.S. Baidak, F.F. Komarov, M.V. Kaverin, N.A. Makhmudov, D.A. Kolesnikov, *Phys. Solid State* **54** No 9, 1882 (2012).
4. A.D. Pogrebnjak, A.A. Bagdasaryan, I.V. Yakushchenko, V.M. Beresnev, *Russ. Chem. Rev.* **83** No 11, 1027 (2014).
5. A.D. Pogrebnjak, D. Eyidi, G. Abadias, O.V. Bondar, V.M. Beresnev, O.V. Sobol, *Int. J. Refract. Met. Hard Mat.* **48**, 222 (2015).
6. A.D. Pogrebnjak, V.S. Ladysev, N.A. Pogrebnjak, A.D. Michaliov, V.T. Shablya, A.N. Valyaev, A.A. Valyaev, V.B. Loboda, *Vacuum* **58** No 1, 45 (2000).
7. A.D. Pogrebnyak, D.I. Proskurovskii, *phys. status solidi a* **145** No 1, 9 (1994).
8. A. Pogrebnjak, A. Lebed, Y. Ivanov, *Vacuum* **63** No 4, 483 (2001).
9. S. Veprek, M.G.L. Veprek-Hejiman, P. Karvankova, J. Prochazka, *Thin Solid Films* **476** No 1, 1 (2005).
10. A.D. Pogrebnjak, V.M. Beresnev, *Nanocoatings, Nanosystems, Nanotechnologies* (Bentham Science Publication: 2012).
11. J. Musil, P. Baroch, P. Zeman, *Plasma Surface Engineering Research and its Practical Applications* (Kerala: Research Signpost: 2008).
12. N. Randall, *Overview of mechanical testing standards* http://www.csm-instruments.com/en/tests-Standards
13. E.V. Berlin, L.A. Seydman, *Ion-plasma Processes in Thin-films Technology* (Moscow: Tchnosphere: 2010).
14. I.I. Aksenov, A.A. Andreev, V.A. Belous, V.E. Strel'nitskyi, V.M. Khoroshyh, *Vacuum-arc: Sourses of Plasma, Coatings Deposition, Surface Modification* (Kyiv: Scientific Thought: 2012).
15. N.A. Azarenkov, O.V. Sobol', V.M. Beresnev, A.D. Pogrebnjak, S.V. Litovchenko, O.N. Ivanov, *Materialsscience Nonequilibrium State of Modified Coating* (Sumy: Sumy StateUniversity: 2013).
16. A.D. Pogrebnjak, I.V. Yakushchenko, A.A. Bagdasaryan, O.V. Bondar, R. Krause-Rehberg, G. Abadias, P. Chartier, K. Oyoshi, Y. Takeda, V.M. Beresnev, O.V. Sobol, *Mater. Chem. Phys.* **147**, 1079 (2014).
17. A.D. Pogrebnjak, S. Bratushka, V.I. Boyko, et.al., *Nucl. Instrum. Meth.* **145** No 3, 373 (1998).
18. A.A. Goncharov, S.N. Dub, A.U. Agulov, *Phys. Met. Metallography* **114** No 1, 95 (2013).
19. P.H. Mayrhofer, C. Mitterer, J.G. Weu, J.E. Greene, I. Petrov, *Appl. Phys. Lett.* **86**, 131909 (2005).
20. J. Musil, *Surf. Coat. Tech.* **207**, 50 (2012).
21. T.N. Koltunowicz, *Acta Phys. Polonica A* **125** No 6, 1412 (2014).
22. T.N. Koltunowicz, P. Zukowski, V. Bondariev, J.A. Fedotova, A.K. Fedotov, *Vacuum* **120**, 44 (2015).
23. P. Zukowski T.N. Koltunowicz, O. Boiko. V. Bondariev, K. Czarnacka, J.A. Fedotova, A.K. Fedotov, I.A. Suito, *Vacuum* **120**, 37 (2015).
24. A.V. Khomenko, I.A. Lyashenko, V.N. Borisyuk, *Ukr. J. Phys.* **54** No 11, 1139 (2009).
25. A.D. Pogrebnjak, A.G. Ponomarev, A.P. Shpak, Yu.A. Kunitskii, *Phys.-Usp.* **55** No 3, 270 (2012).
26. A.A. Goncharov, *Phys. Solid. State* **50**, 168 (2008).
27. I.A. Lyashenko, A.M. Zaskoka, *Tech. Phys.* **60** No 7, 1014 (2015).
28. T.N. Koltunowicz, P. Zukowski, P. Milosavljevic, *J. Alloy. Compd.* **586**, S353 (2014).
29. A.D. Pogrebnjak, A.P. Kobzev, B.P. Gritsenko *J. Appl. Phys.* **87**, 2142 (2000).